PROTEINS: Structure, Function, and Genetics 27:507–516 (1997)

A Model of Insulin Fibrils Derived From the X-Ray Crystal Structure of a Monomeric Insulin (Despentapeptide Insulin)

J. Brange, G. G. Dodson, D. J. Edwards,* P. H. Holden, and J. L. Whittingham
Department of Chemistry, University of York, Heslington, York, England

ABSTRACT **The crystal structure of despentapeptide insulin, a monomeric insulin, has been refined at 1.3 Å spacing and subsequently used to predict and model the organization in the insulin fibril. The model makes use of the contacts in the densely packed despentapeptide insulin crystal, and takes into account other experimental evidence, including binding studies with Congo red. The dimensions of this model fibril correspond well with those measured experimentally, and the monomer–monomer contacts within the fibril are in accordance with the known physical chemistry of insulin fibrils. Using this model, it may be possible to predict mutations in insulin that might alleviate problems associated with fibril formation during insulin therapy.**
Proteins 27:507–516, 1997.

Key words: insulin; despentapeptide; structure; fibrillation; x-ray crystallography

INTRODUCTION

It is now 75 years since insulin was first used in the treatment of diabetes.[1] Since then, many of the biophysical properties of the hormone have been characterized, particularly those associated with self-assembly, fibrillation, crosslinking, and denaturation. These phenomena have, on occasion, presented serious problems in the production and storage of insulin, and its use in therapy. The pharmaceutical industry has largely sidestepped these unfortunate tendencies, and insulin preparations are now characteristically stable and well-behaved. Nonetheless, understanding these phenomena at the molecular level is still important to further improve the use of the hormone in therapy and, just as significantly, to understand more about the nature of the conformational properties and behavior of insulin in solution. One problem, which is as yet unresolved, is the tendency of insulin to form fibrils, particularly in infusion pumps where agitation and elevated temperatures promote their formation.[2] Although a considerable amount of biophysical data pertaining to insulin fibrils is available, as yet the process of fibril formation is not fully understood at the molecular level.

Fibrillation of insulin was first identified in the 1940s[3,4] and was associated with agitation and heating of the solution, and acid pH.[5] Biophysical and electron-microscopic investigations showed that the fibrils were several micrometers long[6,7] and gave some indication of the size of the repeating unit, but they revealed little about the organization of the fibrils. There was additional Raman spectroscopic and Congo red binding studies evidence for the presence of antiparallel β sheet structure.[8,9] When the crystal structure of insulin was solved in 1969,[10] it was revealed that there was an antiparallel β sheet between the B-chain C terminus of the monomers in the dimer. It was a natural assumption that this kind of contact was present in the fiber. Recently, however, it was observed that fibrillation occurred more readily with monomeric insulins in which the B-chain C termini were truncated, such as the despentapeptide and desoctapeptide insulins.[11] Assuming that the native insulin fibrils are similar to those generated by monomeric insulins, this observation implies that fibrils are formed from monomeric insulin rather than dimers and that the β sheet structure in the fibrils is not that which exists between the B-chain C termini in the dimer. It also suggests that the B-chain C terminus does not have a crucial role in fibril formation.

Congo red characteristically binds to antiparallel β strands, which reflects the dye's own internal symmetry, and hence it is widely thought that this structural characteristic will be present in fibrils that bind the dye. The recent experiments of Turnell et al.[9] have demonstrated that Congo red binds to the insulin dimer. This raises the question of how a β sheet structure can occur in the monomeric desocta- and despentapeptide insulin fibrils.

Fibril formation involves a nucleation step in which three or four insulin molecules simultaneously aggregate via their hydrophobic surfaces.[12,13]

Dr. Brange's current address is Biologics Development, Novo Nordisk A/S, 2880 Bagsvaerd, Denmark.
*Correspondence to: Dr. David Edwards, Molecular Simulations Inc., 9685 Scanton Road, San Diego, CA 92121-3752, USA.
Received 28 March 1996; Accepted 14 October 1996

Elevated temperatures provide an entropic driving force for this process. The fibrils are insoluble in most aqueous solutions, but insulin can be regenerated by treatment of the fibrils with very alkaline medium at pH > 11 followed by neutralization.[14] Attempts to inhibit fibril formation include the addition of zinc or calcium to promote normal hexamer assembly, or the introduction of organic or inorganic additives that can behave as impurities.[15] These protocols have met with varied success.

In order to study the fibrillation process, we have carried out structural and modeling studies by using a crystal structure of despentapeptide insulin refined at 1.3 Å resolution. We used a model refined to higher resolution than those already published[16,17] in order to get the best detail of the protein surface structure, particularly the aromatic and aliphatic contacts and the location of water structure. Knowledge of this despentapeptide insulin crystal structure at the atomic level and that of the other native insulin structures provides an opportunity to identify surfaces responsible for fibrillation in the monomeric species. The remarkable advances in modeling technology and theory have now made investigations into such phenomena as fibril formation much more tractable. Moreover, these studies can be related to the knowledge of the structures and the panel of experimental observations. Thus attempts to model the processes in fibrillation can be realistically undertaken.

MATERIALS AND METHODS

X-ray Structure Determination and Refinement of Beef Despentapeptide Insulin

Preparation and crystallization of DPI

Despentapeptide insulin was prepared by enzymatic removal of residues B26–B30 by using the method of Schvachkin et al.[18,19] Crystals of despentapeptide insulin were grown by using the batch crystallization method,[20] the composition of the crystallization solution being as follows: 15 mg despentapeptide insulin, 5.0 ml 0.02 M Tris-HCl/0.05 M trisodium citrate, 1.5 ml 40% saturated ammonium sulfate, 1.5 ml acetone, and 0.1 M citric acid to adjust the pH. This method produced clustered crystals that could be carefully teased apart to give single crystals large enough for data collection. The crystals grew in spacegroup *C2*, with cell dimensions a = 52.70 Å, b = 26.18 Å, c = 51.71 Å, $\alpha = \gamma = 90°$ and $\beta = 93°$, and contain two molecules of the despentapeptide insulin molecule in the asymmetric unit. The solvent content of the crystals was calculated to be 17% by the method of Matthews.[21] This value is among the lowest for any reported protein or macromolecular crystal.

Data collection and data processing

A 1.3 Å dataset was collected on the FAST system at the Daresbury Synchrotron Radiation Source (x-ray wavelength: 0.89 Å) from a single crystal of dimensions 0.15 × 0.20 × 0.30 mm^3. A complete hemisphere of data were collected using an exposure time of 10 seconds per 0.2° frame, and a crystal-to-detector distance of 44 mm. The data were integrated by using a combined profile-fitting algorithm [22]; scaling and merging were carried out by using the CCP4 suite.[23] The dataset consisted of 33,404 measurements, which yielded 16,034 unique reflections (89% complete) with an overall R_{merge} of 0.12; 75% of the data were greater than 3σ. This dataset was then merged with a 1.5 Å dataset from an earlier study[16] to yield a dataset consisting of 31,367 unique reflections (90.7% of possible). This merged dataset was used for refinement.

Refinement

The 1.5 Å despentapeptide insulin structure[16] was used as a starting model for refinement, having removed all of the water molecules. The initial R factor was 0.28, which, after six cycles of restrained least-squares PROLSQ refinement,[23] dropped to 0.25. 46 water molecules were then fitted into $2F_o–F_c$ and $F_o–F_c$ electron density maps using PEAKSEARCH,[23] and given thermal parameters of 40 $Å^2$. Subsequent refinement cycles consisted of coordinate refinement followed by unrestrained isotropic thermal parameter (B) refinement. As the phasing improved, more water molecules were added to the model. At this stage it became apparent that a few of the side chains were disordered. These were omitted from the phasing, and then reintroduced at a later stage in the refinement once their positions were clear in the electron density maps.

In the final stages of refinement all the water molecules were again removed. After three cycles of refinement those waters that appeared in a $2F_o–F_c$ electron density map were reintroduced into the model, taking care to model partially occupied water sites. During further refinement, the water molecule positions and B factors were fixed. To help improve the geometry of the protein model, the contribution from the hydrogen atoms was included in the calculation of the gradients for the protein atoms, although the resolution of the data was not high enough to refine the hydrogen atom positions. In the final model there were 730 protein atoms (including four side chains with dual conformations), 90 water molecules (13 partials). The final R factor was 19% for all data. Other statistics for the 1.3 Å despentapeptide insulin structure, including the refinement restraints, are given in Table I.

RESULTS

Structure Analysis of Beef Despentapeptide Insulin

Despentapeptide insulin consists of two polypeptide chains, comprising residues A1 Gly to A21 Asn

TABLE I. Refinement Restraints and Geometrical Statistics for the Despentapeptide Insulin

Parameter	Target rms	rms Δ for dpi
distances (Å):		
bond (1–2)	0.02	0.01
angle (1–3)	0.04	0.03
planar (1–4)	0.06	0.03
planar group (Å)	0.02	0.01
chiral centre (Å^3)	0.10	0.08
non-bonded (Å):		
single torsion	0.50	0.16
multiple torsion	0.50	0.27
possible H-bonds	0.50	0.31
torsion angles (deg):		
planar	20.0	2.4
staggered	20.0	14.4
orthonormal	20.0	16.3

and B1 Phe to B25 Phe, which are covalently linked by disulfide bridges between residues A7 Cys– B7 Cys and A20 Cys–B19 Cys. There is a third, intrachain disulfide bridge between residues A6 Cys and A11 Cys. The protein has the same secondary structure elements as its insulin precursor, namely, α helices spanning residues A1 Gly–A8 Thr, A12 Ser–A21 Asn and B9 Ser–B19 Cys, and extended chain regions from A9 Ser to A11 Cys, B1 Phe to B8 Gly and B21 Glu to B25 Phe. Inspection of the Ramachandran plot (not shown) reveals that there are no unfavorable ϕ/ψ angles in the protein structure. As is to be expected in such a tightly packed crystal, the thermal parameters for the atoms are generally relatively low, 90% being in the range 3 to 20 Å^2. Only two amino acids have main-chain B values greater than 20 Å^2 and only five side chains have greater than 30 Å^2. Equally the thermal parameters for the water molecules are generally lower than is usually the case for proteins.

There are two molecules of despentapeptide insulin within the crystallographic asymmetric unit. These have the same orientation and are related by a translation of approximately half a unit cell in the direction of the crystallographic *c* axis. The two molecules make close-packing interactions with molecules of other asymmetric units rather than with each other, there being a small solvent channel between the two. The two molecules are similar but not identical owing to crystal packing restraints (Fig. 1). The overall root-mean-square (rms) difference between the mainchain atoms is 0.6 Å, and most of this difference is accounted for by differences in the A chains, which have a mainchain rms difference of 0.5 Å. When the two B chains are compared, the central B9–B19 α helices are almost identical, having a main-chain rms difference of 0.2 Å; however, at the B-chain N and C termini there are differences of 1.5–2.3 Å. Comparison of the DPI crystal structure with the 1.5 Å structure determined in Beijing[17] suggest that the molecules are essentially the same in the two crystalline forms (Liang Dongcai, private communication). An exact comparison cannot be made, since the coordinates for the Chinese structure are not available.

The two despentapeptide insulin molecules bear most resemblance to molecule 1 of 2Zn pig insulin dimer.[24] Comparison of molecules 1 and 2 of despentapeptide insulin with molecule one of 2Zn pig insulin shows the similarity is greatest in the helical region between residues B9 and B19. For this reason the molecules have been least-squares aligned on residues B1–B19 to illustrate the differences in other parts of the molecules (Fig. 1).It can be seen that the conformation at the B-chain N terminus of despentapeptide insulin is very different from that of 2Zn pig insulin, folding away from the molecule to facilitate crystal packing interactions (see below). There is a clear movement of the A-chain N-terminal helix toward the B-chain C terminus of between 2.2–2.9 Å, a conformational change that is probably compensating for the loss of the contacts with B26–B30. This rearrangement may also be necessary to accommodate the changes at the B-chain N terminus. At the C terminus of the B-chain residue B25 Phe in despentapeptide insulin is folded away from the main body of the molecule, unlike that in the 2Zn pig insulin molecule. In this conformation the B25 Phe main chain and side chain do not make contact with the rest of the monomer and even more of the nonpolar core is exposed.

Crystal Packing in Despentapeptide Insulin

The packing of the two DPI molecules in the crystal is shown in Figure 2. The lettering for the crystallographic cell axis is given in bold type to distinguish it from the lettering for the axes in the model fibril. In the crystal there are two principal sets of packing interactions, which are in the direction of the crystallographic *a* and the *c* axes (as highlighted in Fig. 2). In the *a* direction adjacent to symmetry-related molecules form antiparallel β strands between residues B1 and B5 and their crystallographic twofold equivalent (Fig. 3). These strands are roughly parallel to the *c* axis. There are four peptide amide–carbonyl bonds made between the two strands; two across the twofold axis N B3 Asn to O B2 Val (2.9 Å), and one from either end of the strand at the N termini of B1 Phe to O B4 Glu (3.0 Å). van der Waals contacts between the aromatic side chains of B1 Phe and B16 Tyr, and residues B5 His and B10 His of adjacent molecules add to the crystal packing interactions in this direction. These interactions presumably constitute a large driving force in the crystallization of despentapaptide insulin.

The close-packing interactions in the direction of *c* are provided by two B9–B19 α helices of adjacent molecules that are related to each other by two

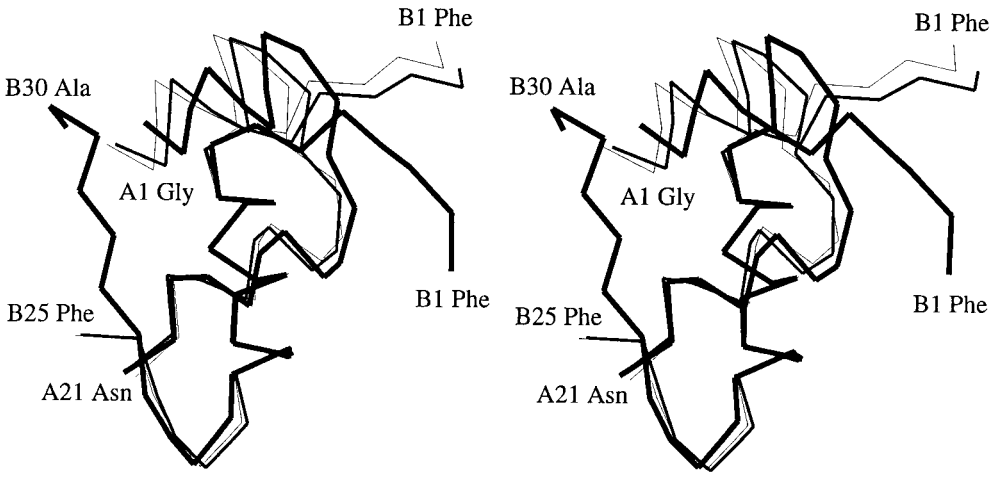

Fig. 1. Stereo view showing an overlap of the Cα atoms of molecule one of 2Zn pig insulin (bold lines) with molecules one and two of DPI (fine and medium lines, respectively). The three molecules were superposed by least-squares fitting the main chain atoms of residues B9 to B19. Chain termini are labeled.

twofold screw symmetry. This results in the burial of about 710 Å^2 of hydrophobic surface, into which project B24 Phe and B25 Phe (Fig. 4). Both B24 and B25 are further shielded by the twofold related dimer (not shown). This arrangement results in a hydrophobic cavity, which effectively buries the nonpolar residues in DPI exposed by the chemical removal of residues B26–B30 from the native insulin molecule (Fig. 5). There are few crystal packing interactions in the crystallographic *b* direction apart from the van der Waals contact between the aromatic side chains of residues A14 Tyr and A19 Tyr of adjacent molecules.

Water in the DPI Crystal

Although DPI molecules are densely packed in the crystal, there are solvent channels which lie parallel to the *ab* plane of the unit cell (Fig. 2). It is notable that 75% of water molecules belong to a first layer hydration shell; hence there is no bulk solvent in DPI, most of the waters being directly hydrogen-bonded to protein atoms. The clustering of waters around hydrophobic residues forming cages, which is observed in some high-resolution structures, for instance, insulin and crambin,[25] is not seen in the DPI crystal, presumably owing to the lack of space in the lattice.

MODELING FIBRIL CONTACTS

The crystal packing of the nonpolar surfaces in the direction of the crystallographic *c* axis was considered to be the initiating direction of fibril formation because of the large and readily accessible nonpolar regions buried by these interactions. A chain of insulin monomers was generated by using this contact and reproducing the burial of the hydrophobic surfaces on the "front" and "back" of the DPI monomer (Fig. 6). This arrangement brings into van der Waals contact the aliphatic residues A13 Leu, B6 Leu, B14 Ala, B17 Leu, and B18 Val from one molecule with A2 Ile, As Val, B11 Leu, and B15 Leu from another. The surfaces buried at this interface are all aliphatic. They exhibit a great degree of complementarity both in terms of their chemistry and their shape. Analysis of these aliphatic interfaces shows they are packed together tightly with no cavities in which buried water molecules might sit. The high resolution of the data have allowed the intricate and complementary contacts at the interface to be defined with good accuracy (~0.1 Å), and make it possible to be confident about the nature of the aliphatic packing and the absence of water. The modeling leads to a proposal for an insulin fibril with dimensions 40 Å by 25 Å and a unit repeat of 20 Å, that is, the dimensions of an insulin monomer. The second set of contacts involved in fibril formation we consider to be the antiparallel β sheet structure between the B1 Phe–B5 His residues, which run along the *a* axis direction. In the fibril these are referred to as the [a] contacts and they are roughly perpendicular to the model [c] contacts as described above (Fig. 7). These five residues provide the only van der Waals contact in this direction of fibril packing. As well as the contacts observed between opposing strands, the side chain of B4 Glu makes loose van der Waals interactions with the main chain of B21 Glu and B22 Arg in the adjacent molecule. In addition, B5 His from one molecule sits above the B-chain C terminus of an adjacent molecule and makes a ring-stacking interaction with the side chain of B10 His from this molecule. We do not

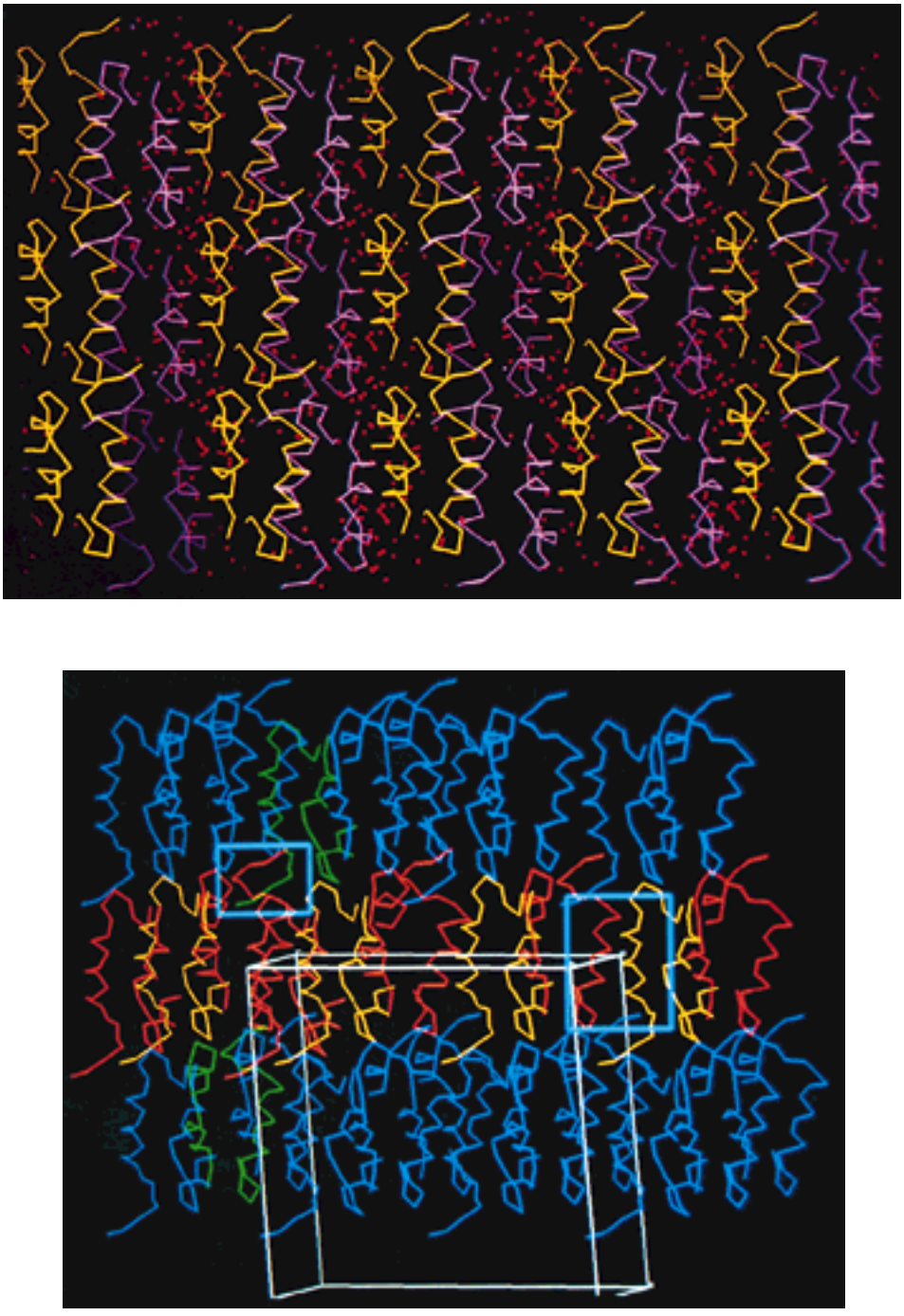

Fig. 2. View of the DPI crystal perpendicular to the crystallographic *b* axis. **Top:** Symmetry-related DPI molecules (Cα atoms only) in yellow and purple, interspersed by water molecules (red dots). The main solvent channels in the DPI crystal run parallel to the crystallographic *a* axis, vertically as shown. **Bottom:** The two main classes of packing described in the text are highlighted by boxes. Alternately green and red molecules are used to highlight packing in the *a* direction and red and yellow molecules in the *c* direction.

consider that these weaker interactions are significant in the generation of the fiber. Packing of DPI molecules in a third direction in the crystal, *b*, is not likely to represent fibril contacts, since here intermolecular interactions are most loose and hydration most developed (Fig. 2).

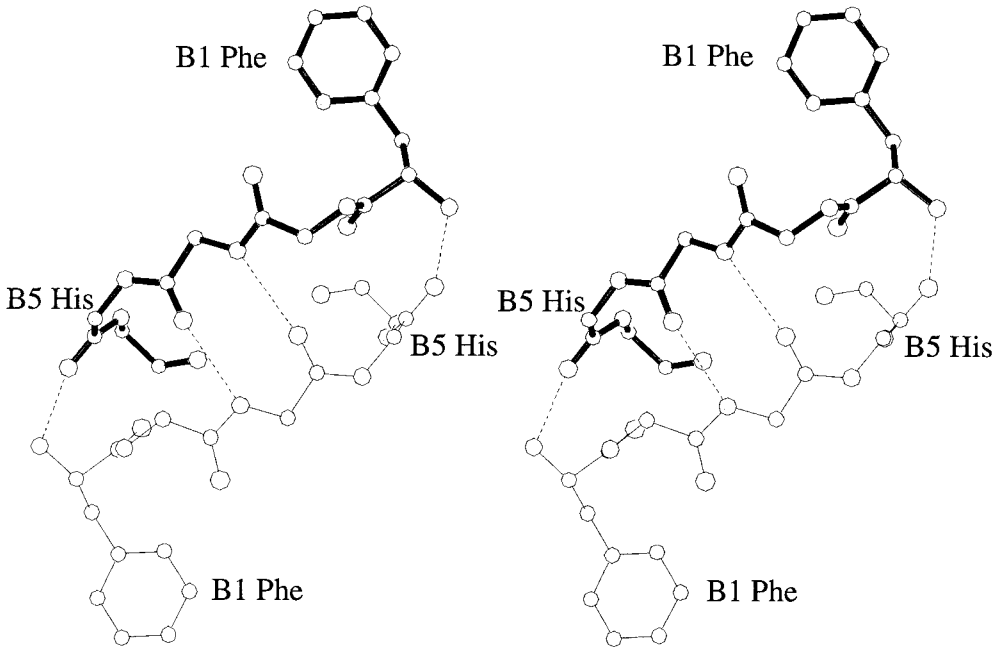

Fig. 3. Stereo view showing crystal packing interactions in the direction of the crystallographic *a* axis. The antiparallel β strands are formed between residues B1–B5 of symmetry-related DPI molecules (in bold and fine lines) in the crystal. Hydrogen bonds are represented by dotted lines.

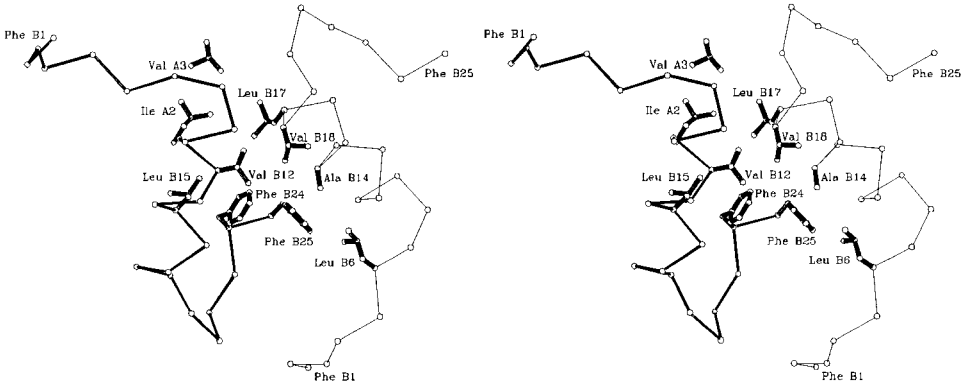

Fig. 4. Stereo view showing crystal packing interactions along the crystallographic *c* axis. Two symmetry-related molecules (in bold and fine lines) pack to form a hydrophobic pocket into which residues B24 and B25 project. Other hydrophobic residues whose side chains line this pocket are also shown highlighted in bold. The A chains of both molecules have been removed for clarity.

DISCUSSION AND CONCLUSIONS

Structural studies on this monomeric insulin show that, apart from the loss of the β sheet between residues B26–B30, the despentapeptide insulin molecule retains all the secondary and tertiary structure characteristics of the native hormone. Consequently, both the hydrophobic dimer-forming and hexamer-forming surfaces of insulin are also present in DPI as well-defined structures,[16] the dimer-forming surface being modified by the removal of residues B26–B30. The greater tendency for despentapeptide and desoctapeptide insulin to form fibrils is probably associated with the extra hydrophobic area revealed when the B-chain C terminus is removed. In the despentapeptide insulin crystal structure the two hydrophobic surfaces are tightly packed against one another resulting in dense crystal packing and very low solvent content. Electron microscopy[7] and x-ray diffraction[26] suggest that the fibrils have a uniform cross section with dimensions of about 30 Å × 50 Å; these match the DPI monomer. The contacts observed in the DPI crystal in the *a* and *c* directions have the appropriate character for fibril development. We propose that these interactions are

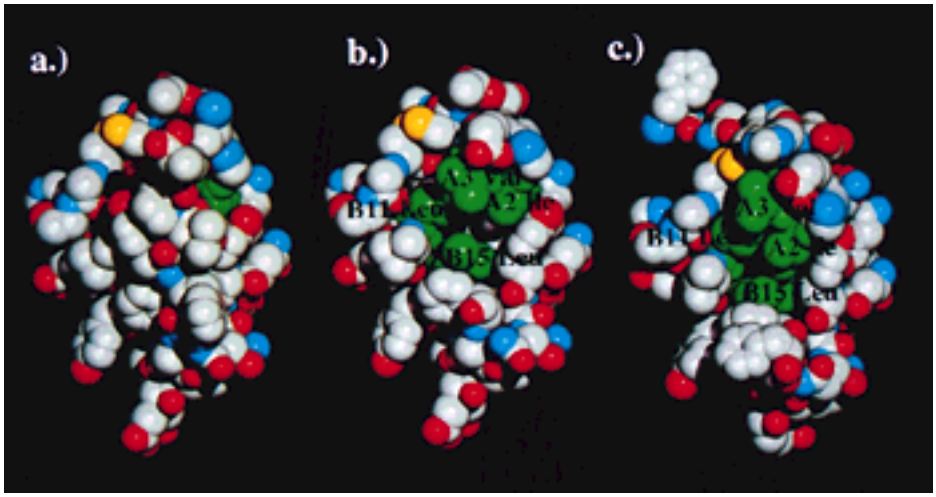

Fig. 5. van der Waals representation. **a:** The dimer-forming face of the 2Zn pig insulin. **b:** The same face with residues B26 to B30 removed, revealing the hydrophobic side chains of residues A2 Ile, A3 Val, B11 Leu, and B15 Leu (in green). **c:** The corresponding face in the DPI structure. Hydrophobic residues discussed in the text are highlighted.

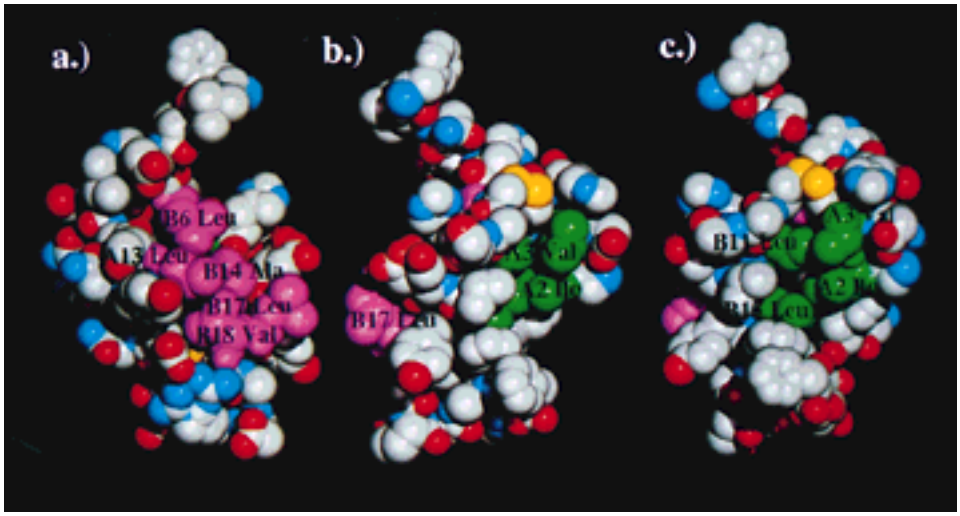

Fig. 6. **a,c:** van der Waals representations of the DPI molecule showing the two hydrophobic faces in pink (residues A13 Leu, B6 Leu, B14 Ala, B17 Leu, and B18 Val) and green (residues A2 Ile, A3 Val, B11 Leu, and B15 Leu) used to generate the fibril (Figures a. and c.). **b:** The relative positions of the two surfaces on the DPI molecule.

also responsible for the growth of native insulin fibrils.

In the fibril it is clear that in the [c] direction assembly of the fibril will be driven by nonpolar and entropic effects. The model presented requires the simultaneous assembly of three molecules to shield the nonpolar surfaces on one monomer. This is consistent with previously observed experiments.[12,13]

Raman spectra[8] and studies of the binding of Congo red to insulin fibrils[9] tend to support the presence of an antiparallel β sheet in the insulin fiber. The crystal structure of DPI provides an alternative antiparallel β sheet contact made by the N-terminal residues of the B chain. This sheet is perpendicular to the principal fiber axis, as required from the spectroscopic observations,[27] and is a favorable contact through which bundles of fibrils may develop from individual fibrils.[6]

The development of the fibril in the third [b] direction has not been modeled. The DPI crystal structure does not exhibit packing characteristics suggestive of fibril growth in this direction. Instead, crystal contacts in this direction are mediated by large solvent channels. Examination of the [b] surface in the fibril model reveals the presence of large groups of hydrophobic residues, which would become buried upon propagation of the fibril in this third direction (Fig. 8). The location of the B-chain C-terminal residues in the native insulin fiber is not, however, identified with any certainty. These resi-

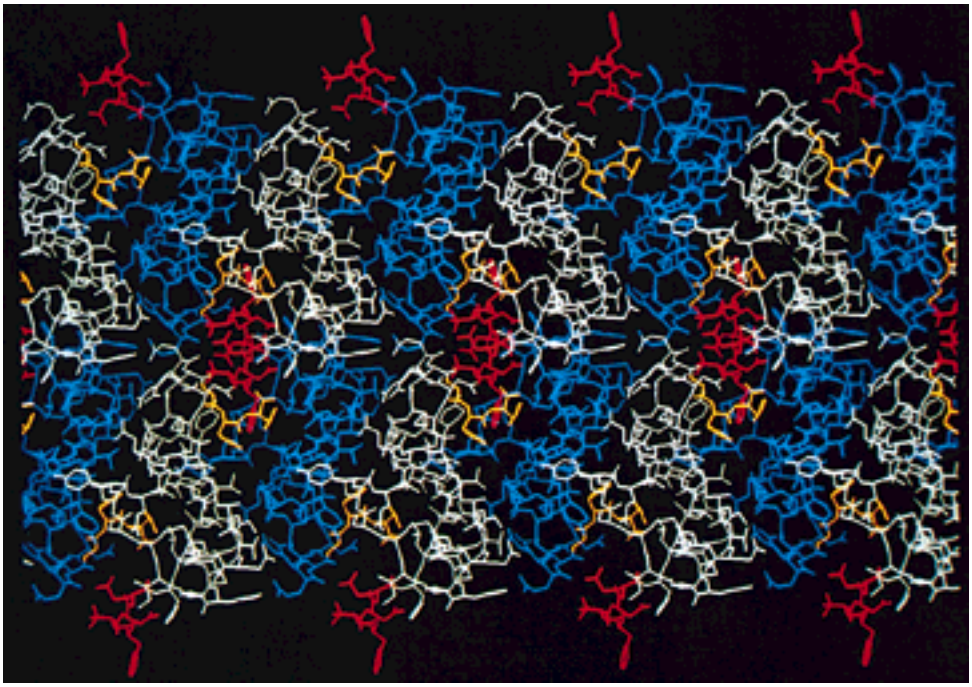

Fig. 7. Two strands of the modeled DPI fibril. Adjacent molecules are shown in alternate colors—blue and pale green—running in a direction that corresponds to the *c* axis in the DPI crystal. The B1–B5 β strands are highlighted in red and residues B23–B25 are highlighted in yellow.

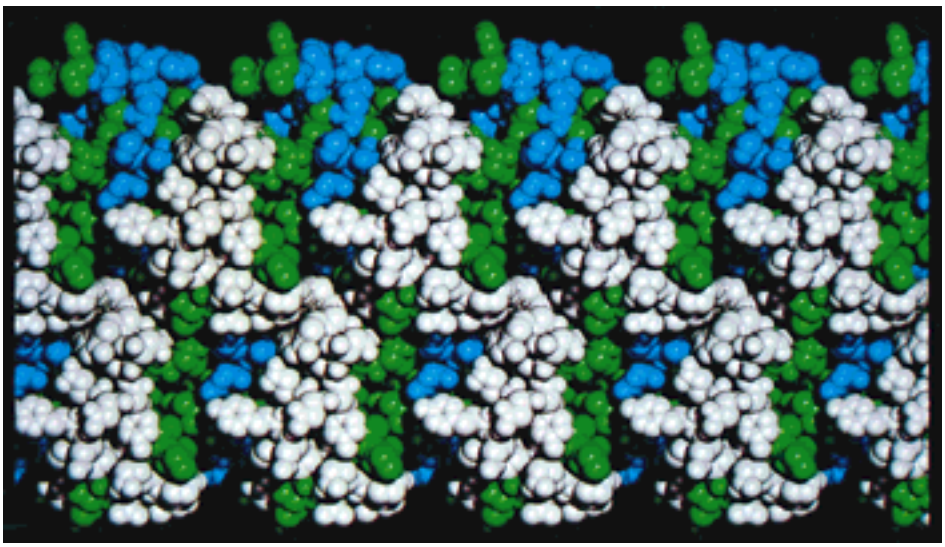

Fig. 8. van der Waals representation of the unmodeled [b] surface of the DPI model fibril. Alternate molecules are blue and green. Hydrophobic residues are highlighted in pale green.

dues, being flexible, may themselves pack favorably against this remaining exposed monomer surface [b] as illustrated in Figure 9.

However, the contacts which dominate fibril formation must be made by those residues that are not in the B-chain C terminus, since both DPI and DOI

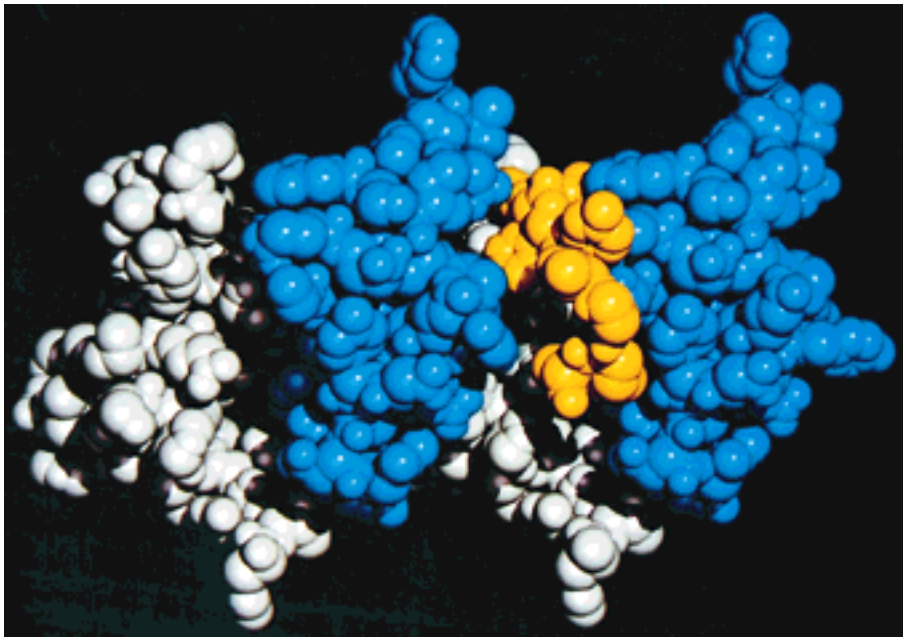

Fig. 9. Four adjacent molecules of the DPI model fibril (blue and pale green) showing the B-chain C terminus in yellow (residues B23–B30) modeled onto the hydrophobic surface.

form fibrils. It follows from this that in native insulin the residues B23 Gly–B30 Thr are displaced during fibril formation. Indeed the more rapid fibrillation of the DPI and DOI suggests that the aliphatic contacts alone made by these surfaces drive fibril formation. Support for the displacement of the B-chain C-terminal residues (B23–B30) in fibrillation also comes from the behavior of proinsulin and the miniproinsulin (A1–B30 crosslinked by two amino acids). Proinsulin fibrillates to a greatly reduced extent, the dipeptide crosslinked insulin fibrillates even less; that is, fibril formation is closely linked to the flexibility (or displacement) of the B-chain C-terminal residues.[11]

It is possible to probe the role of individual amino acids on the candidate fibril-forming surfaces by site-directed mutation experiments. It is feasible that mutations of some of the hydrophobic residues that form close-packing interactions in the model fibril, such as A13 Leu, B14 Ala, and B17 Leu, may inhibit fibril formation without undermining the structure of the molecule. Likewise, removal of some of the residues involved in β sheet formation, B1 Phe and B2 Val, could limit fibril formation. Studies to characterize the DOI and DPI fibrils by chemical and structural methods are planned, and their similarity, or differences, to the native insulin fibers established. The role of the β sheet interactions made by residues B1 Phe–B4 Glu in encouraging fibril growth will also be investigated by using insulins truncated at the B-chain N terminus. This research will, we hope, put fibril formation in insulin on a firm molecular basis and perhaps suggest parallels that will apply to the general phenomenon of amyloid deposits.

ACKNOWLEDGMENTS

We thank Miroslav Papiz at the Daresbury SRS for guidance with the DPI project, and Eleanor Dodson and Marek Brzozowski for help and useful discussions. Novo Nordisk and the BBSRC are gratefully acknowledged for financial support.

REFERENCES

1. Banting, F.G., Best, C.H. Pancreatic extracts. J. Lab. Clin. Med. 7:464–472, 1922.
2. Lougheed, W.D., Woulfe-Flanagan, H., Clement, J.R., Albisser, A.M. Insulin aggregation in artificial delivery systems. Diabetologia 19:1–9, 1980.
3. Langmuir, I., Waugh, D.F. Pressure-soluble and pressure-displaceable components of monolayers of native and denatured proteins. J. Am. Chem. Soc. 62:2771–2793, 1940.
4. Waugh, D.F. The properties of protein fibers produced reversibly from soluble protein molecules. Am. J. Physiol. 133:P484–P485, 1941.
5. Waugh, D.F. A fibrous modification of insulin. I. The heat precipitation of insulin. J. Am. Chem. Soc. 68:247–250, 1946.
6. Farrant, J.L., Mercer, E.H. Electron microscopical observations of fibrous insulin. Biochim. Biophys. Acta 8:355–359, 1952.
7. Glenner, G.G., Eanes, E.D., Bladen, H.A., Linke, R.P., Termine, J.D. A comparison of native amyloid with synthetic protein fibrils. J. Histochem. Cytochem. 22:1141–1158, 1974.

8. Yu, N.T., Jo, B.H., Chang, R.C.C., Huber, J.D. Single-crystal Raman spectra of native insulin: Structures of insulin fibrils, glucgon fibrils and intact calf lens. Arch. Biochem. Biophys. 160:614–622, 1974.
9. Turnell, W.G., Finch, J.T. Binding of the dye Congo red to the amyloid protein pig insulin reveals a novel homology amongst amyloid-forming peptide sequences. J. Mol. Biol. 227:1205–1233, 1992.
10. Adams, M.J., Blundell, T.L., Dodson, E.J., Dodson, G.G., Vijayan, M., Baker, E.N., Harding, M.M., Hodgkin, D.C., Rimmer, B., Sheat, S. Structure of 2 zinc insulin crystals. Nature 224:491–495, 1969.
11. Brange, J., Hansen, J.F., Havelund, S., Melberg, S.G. Studies of the insulin fibrillation process. In "Advanced Models for the Therapy of Insulin Dependent Diabetes." Brunetti, P., Waldhäusl, W.K. (eds.). New York: Lippincott-Raven, 1987:85–90.
12. Waugh, D.F., Wilhelmson, D.F., Commerford, S.L., Sackler, M.L. Studies on the nucleation and growth reactions of selected types of insulin fibrils. J. Am. Chem. Soc. 75:2592–2600, 1953.
13. Waugh, D.F. A mechanism for the formation of fibrils from protein molecules. J. Comp. Physiol. 49(Suppl. 1):145–164, 1957.
14. Waugh, D.F. Regeneration of insulin from insulin fibrils by the action of alkali. J. Am. Chem. Soc. 70:1850–1857, 1948.
15. Brange, J. Skelbaek-Pedersen, B., Langkjaer, L., Damgaard, U., Ege, H., Havelund, S., Heding, L.G., Jøgensen, K.H., Lykkeberg, J., Markussen, J., Pingel, M., Rasmussen, E. "Galenics of Insulin: The Physico-chemical and Pharmaceutical Aspects of Insulin and Insulin Preparations." Berlin: Springer-Verlag, 1987.
16. Bi, R.-C., Cutfield, S.M., Dodson, E.J., Dodson, G.G., Giordano, F., Reynolds, C.D., Tolley, S.P. Molecular-replacement studies on crystal forms of despentapeptide insulin. Acta Crystallogr. B39:90–98, 1983.
17. Jinbi, D., Meizhen, L., Junming, Y., Dongcai, L. Refinement of the structure of despentapeptide (B26–30) insulin at 1.5 Å resolution. Sci. Sin. Ser. B 30:55–65.
18. Schvachkin, Y.P., Schmeleva, G.A., Krivtsov, V.F., Fedotov, V.P., Ivanova, A.I. Isolation and properties of des-(pentapeptide-B26–B30)-insulin. Biokhimiya 37:966–973 (1972).
19. Holden, P.H. D. Phil. X-ray studies of modified insulins. Thesis, University of York, UK, 1991.
20. Harding, M.M., Hodgkin, D.C., Kennedy, A.F., O'Connor, A.,, Weitzmann, P.D.J. The crystal structure of insulin. II. An investigation of rhombohedral zinc insulin crystals and a report of other crystalline forms. J. Mol. Biol. 16:212–226, 1966.
21. Matthews, B.W. Solvent content of protein crystals. J. Mol. Biol. 33:491–497, 1968.
22. Helliwell, J.R., Machin, P.A., Papiz, M.Z. Computational aspects of protein crystal data analysis. In "Proceedings of the Daresbury Study Weekend, SERC Daresbury, UK." Papiz, M.Z., Andrews, S.J. (eds.). 1987:181–190.
23. Collaborative Computational Project, Number 4. The CCP4 suite: Programs for protein crystallography. Acta Crystallogr. D50:760–763, 1994.
24. Baker, E.N., Blundell, T.L., Cutfield, S.M., Dodson, E.J., Dodson, G.G., Crowfoot Hodgkin, D.M., Hubbard, R.E., Isaacs, N.W., Reynolds, C.D., Sakabe, K., Sakabe, N., Vijayan, N.M. The structure of 2zinc piginsulin crystals at 1.5 Å resolution. Phil. Trans. R. Soc. Lond. B319:369–456, 1988.
25. Teeter, M.M., Roe, S.M., Heo, N.H. Atomic resolution (0.83 Å) crystal-structure of the hydrophobic protein Crambin at 130 K. J. Mol. Biol. 230:292–311, 1993.
26. Burke, M.J., Rougvie, M.A. Cross-*b* protein structures. I. Insulin fibrils. Biochemistry 11:2435–2439, 1972.
27. Ambrose, E.J., Elliott, A. Infra-red spectroscopic studies of globular protein structure. Proc. R. Soc. (Lond.) 208:75–90, 1951.